Journal of Materials Chemistry A

Accepted Manuscript

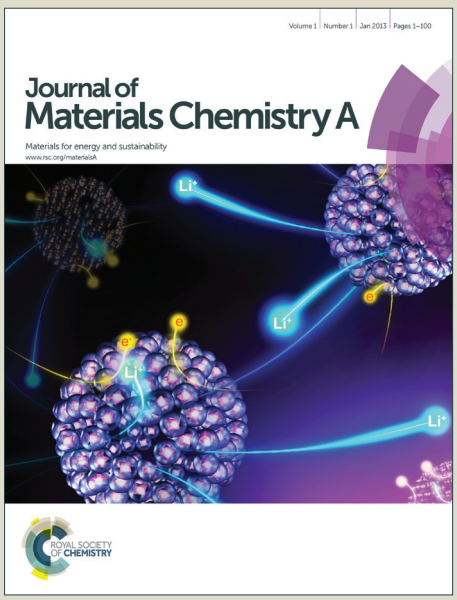

ROYAL SOCIETY OF CHEMISTRY

www.rsc.org/materialsA

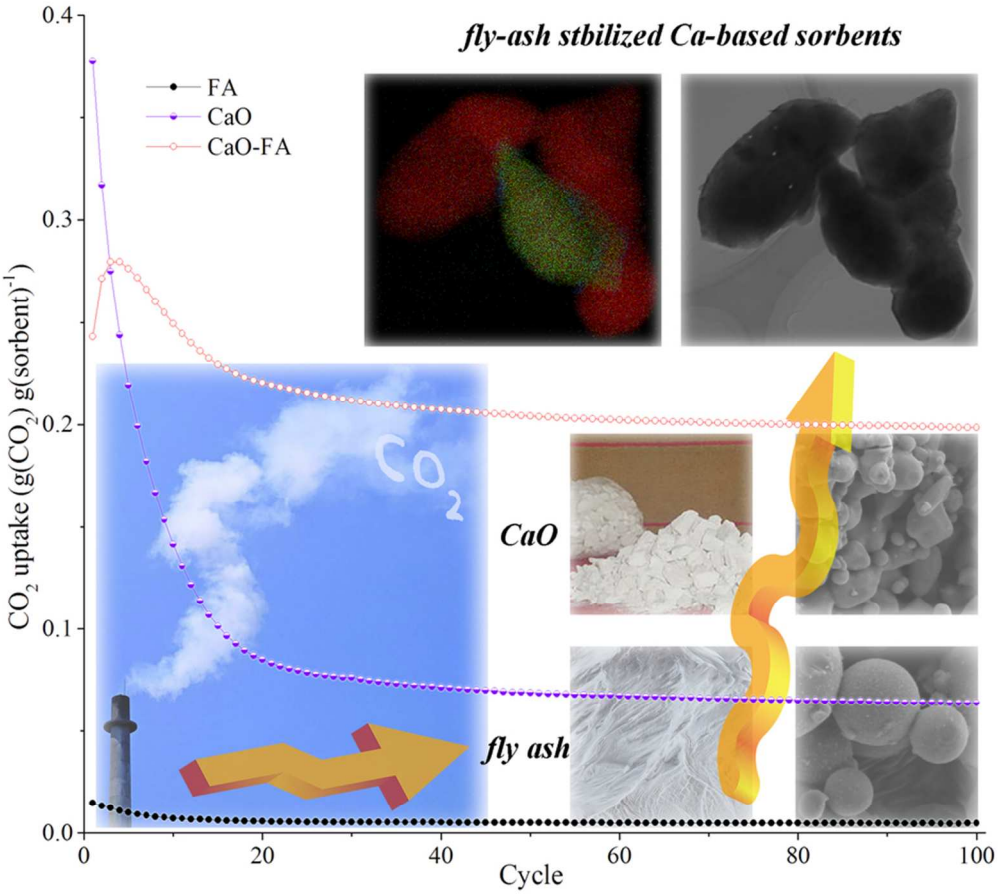

Highly stabilizing effect of fly ash on CaO-based sorbents under severe calcination conditions
40x36mm (600 x 600 DPI)

Article type: Full Paper

A green and scalable synthesis of highly stable Ca-based sorbents for CO_2 capture

Feng Yan, [a] *Jianguo Jiang,* [a,b,c*] *Ming Zhao,* [a] *Sicong Tian,* [a] *Kaimin Li,* [a] *Tianran L i* [a]

[a] School of Environment, Tsinghua University, Beijing 100084, China.

[b] Key Laboratory for Solid Waste Management and Environment Safety, Ministry of Education, Beijing 100084, China.

[c] Collaborative Innovation Center for Regional Environmental Quality, Tsinghua University, Beijing 100084, China

***Corresponding author:**

Prof. Dr. Jiang Jianguo (School of Environment, Tsinghua University, Beijing 100084, China.)

Tel.: +8610-62783548 Fax: +8610-62783548

E-mail address: jianguoj@tsinghua.edu.cn

Key Words: (CO_2 capture, Ca-based sorbents, fly ash, sintering resistance, refractory stabilizer)

Abstract: High-temperature sorption of CO_2 via calcium looping is a promising technology for implementation of carbon capture and storage (CCS). However, the rapid deactivation of CaO sorbents due to sintering, is currently the major drawback of this technology. We, for the first time, report an economical and environmentally benign strategy to reduce sintering by adding fly ash, a waste stream of coal-fired plants, into Ca-based sorbents through a simple dry process. The as-synthesized sorbents were tested in TGA and showed an extremely high stability under the most severe multi-cycle conditions (calcined at 920ºC in pure CO_2). Upon 100 cycles, its CO_2 capture capacity was 0.20 g(CO_2) g(sorbent)$^{-1}$, and the average deactivation rate was only 0.18% per cycle. The most possible stabilization mechanism was discussed on basis of a range of characterizations including N_2 physisorption, SEM, TEM (coupled with EDX mapping) and XRD; it was concluded that stable and refractory gehlenite ($Ca_2Al_2SiO_7$) particles were formed and evenly dispersed around CaO crystal grains during calcination at 950ºC, leading to sintering resistance. This strategy achieved superior enhancement to the cyclic stability of Ca-based sorbents as well as reuse of industrial solid waste, and is thus a green technology for scaled-up CO_2 capture.

1. Introduction

The concentration of CO_2 in the atmosphere has been increasing from a pre-industrial level of 280 ppm to its current level of 391 ppm,[1] which is most likely associated with climate change according to the 5th assessment report of the Intergovernmental Panel on Climate Change (IPCC). Considering the continuous use of fossil fuels, a most promising mid-term strategy of CO_2 capture and storage (CCS)[2] was proposed to limit CO_2 emission. However, the cost of available CO_2 capture technology, amine scrubbing, is extremely high at approximately 54 \$ $t(CO_2)^{-1}$, much higher than the market acceptance level.[3] Thus, it is imperative to develop efficient and cost effective alternative technologies.

A promising CO_2 capture technology is based on the reversible carbonation and calcination of CaO, which was first introduced in the framework of CCS in 1999.[4] Owing to the high theoretical capacity of 0.78 $g(CO_2)$ $g(CaO)^{-1}$ and the low costs of CO_2 avoided (as low as 18 \$ $t(CO_2)^{-1}$),[5] natural Ca-based sorbents such as limestone and dolomite seem to be attractive.[6] However, the CO_2 capture capacity of CaO derived from natural sources decreases rapidly over multiple cycles because of sintering and attrition,[7] leaving a residual activity conversion of 10%.[8] Thus, different pre-treatments, such as hydration[9] or thermal treatment,[10] are known to improve the stability of limestone; alternatively, synthetic CaO from various calcium precursors has been used to obtain high surface areas and favorable microporous structures.[11] Even so, severe sintering still exists in these unsupported materials,[12] leading to a similar decay of limestone under realistic calcination conditions (temperature > 900ºC and pure CO_2 atmosphere).[13]

A more effective strategy was proposed to stabilize CaO using a support with a high Tammann temperature (T_T, an empirical temperature where sintering becomes active), such as Al_2O_3,[14-16] MgO,[17, 18] SiO_2,[19, 20] ZrO_2,[21, 22] TiO_2[23, 24] or Y_2O_3.[25] Various wet-process methods, including carbon templating,[14] so-gel,[26, 27] co-precipitation,[15, 17] wet mixing[18] and hydration,[28] have been used to uniformly disperse the inert support material and effectively minimize sorbent sintering. At this time, studies have focused on the use of simple synthesis techniques and inexpensive support materials. A potential technique is the dry-process method with a direct solid-state reaction between CaO and the support materials. Valverde et al.[19] synthesized SiO_2-stabilized, Ca-based sorbents containing 85 wt% CaO by mechanical mixing of $Ca(OH)_2$ and fumed silica with the nanostructure, and the capture capacity was improved from 0.10 to 0.18 $g(CO_2)$ $g(sorbent)^{-1}$ after 100 cycles

(calcination at 850ºC in N_2 atmosphere). Additionally, solid waste sources containing SiO_2 and Al_2O_3, such as kaolin,[29] rice husk ash,[30] and cement,[31] were recently used as a cheaper support material to stabilize the CaO structure, and all sorbents showed a better cyclic stability with supports (Table 2). However, considering the cost of production, raw materials and transportation, a highly efficient sorbent for realistic CO_2 capture is still a research hotspot.

Coal is the world's most important fuel for electricity generation accounting for ~40% of the global carbon emissions.[1] Meanwhile, fly ash (FA) generated in coal-fired power plant in China reached up to 532 million tons by the year 2013, which can cause serious environmental hazards.[32] Thus, we first report the stabilizing effect of fly ash on Ca-based sorbents for cyclic CO_2 capture. Several characterization techniques were used to examine the properties of Ca-based sorbents both before and after the reaction. Subsequently, long-term (100 cycles) cyclic CO_2 sorption tests were performed to investigate the stability of the synthetic sorbents under the severe cyclic carbonation-calcination conditions. This approach could be used both for high-value utilization of fly ash without long distance transport and reduction of CO_2 emissions from coal-fired fired power plants through on-site CO_2 capture.

2. Experimental

2.1 Sorbent preparation.

A typical low-calcium fly ash (FA-0h) from a coal-fired power plant (Hebei, China) was used as a support material to prepare the Ca-based sorbents. The fly ash was calcined for 2 h at 900ºC in an air atmosphere to remove organic components, after which the preheated fly ash was sieved to obtain particle sizes of less than 74 μm (FA-2h, Fig. S1). Although CaO decomposed from calcium acetate exhibited relatively higher pore volumes and was a better calcium source,[11] a common CaO (AR, 98 wt%, China) was used as a calcium precursor, considering the high cost of calcium acetate. The CaO powder (9 g) was physically dry-mixed with the pretreated fly ash (1 g) in agate mortar for 10 min, after which the mixture was thermally treated in a muffle furnace at 950ºC in an air atmosphere to obtain Ca-based, fly-ash-stabilized sorbents (CaO-FA). The duration of thermal treatment varied from 0 to 12 h; thus, the sorbents were designated based on their thermal treatment conditions; e.g., CaO-FA-2h for 2 h of thermal treatment.

2.2 Characterization.

The particle size distributions of samples were examined using a dry powder laser particle sizer (Beckman coulter, LS 13320, USA). Nitrogen adsorption-desorption isotherms of nanoparticles at 77 K were collected on a gas adsorption analyzer (Micrometrics Instrument, ASAP2020 HD88, America); all samples were degassed in a vacuum at 90ºC for 1 h a nd at 350ºC for 2 h be fore measurement. BET surface area was calculated using the Brunauer–Emmett–Teller (BET) method over P/P_0 = 0.05-0.25, and the total pore volume was calculated from the adsorbed volume at P/P_0 = 0.99. The pore size and pore distributions were derived from the desorption branch of the N_2 isotherm using the Barrett-Joyner-Halenda (BJH) method. Sorbent morphology was characterized by scanning electron microscope (SEM, Zeiss Merlin Compact, Germany) using a 5-kV electron beam and a field emission transmission electron microscope (TEM, JEM-2010F, Japan) with a 200-kV electron beam. Elemental Ca, Si and Al distribution mapping was performed using JEM-2010F fitted with an electron energy loss spectroscopy (EELS) detector, and the element content was also measured using JEM-2010F equipped with an Oxford energy-dispersive spectrometer (EDS). X-ray fluorescence (XRF) was performed to analyze the composition and content of elements in the sorbents using an XRF-1800 analyzer (Shimadzu, XRF-1800, Japan). The mineral composition of the sorbents was recorded using high-resolution X-ray diffraction (XRD, Siemens D8 Advance, Germany) with Cu-Kα radiation (λ = 0.15418 nm) in the 2θ range of 10-90º (scanning rate of 6º min^{-1}).

2.3 Cyclic CO_2 capture.

The CO_2 capture capacity of the Ca-based sorbents was determined using a thermal gravimetric analyzer (TGA, Mettler-Toledo, TGA/DSC 2, Switzerland) with a high-sensitivity balance (<0.1 μg). A small quantity (8-10 mg) of the sorbents were placed in a 150-μL alumina pan and heated (30°C min^{-1}) to the carbonation temperature (800ºC) under a flow of 60 mL min^{-1} N_2. Additionally, a constant flow of 20 mL min^{-1} N_2 was used as a protective flow over the micro-balance during the experiment. When the carbonation temperature was reached, the sorbents were subjected to a flow of 60 mL min^{-1} CO_2 for 25 min. Subsequently, the temperature was increased to 920°C (60°C min^{-1}) and the calcination reaction was performed at 920°C under an atmosphere using 100 vol.% CO_2 (60 mL min^{-1}) for 5 min. After calcination a new cycle was started by reducing the reaction temperature to 800°C (60°C min^{-1}) and keeping the reactive flow of 60 mL min^{-1} CO_2. The

carbonation-calcination cycle was repeated 30-100 times for each sorbent. The cyclic CO_2 uptake of the sorbents (X, g(CO_2) g(sorbent)$^{-1}$) was calculated from the continuously recorded weight changes during carbonation and calcination: $X_N = m_{1N} - m_{2N}/m_0$, where m_0, m_{1N} and m_{2N} (mg) refer to the initial sorbent mass and the sorbent mass after N cycles of carbonation and calcination, respectively.

3. Results and Discussion

3.1 Characterization of supports and sorbents

The fly ash possessed type II N_2 adsorption–desorption isotherms (Fig. S2), as classified by the International Union of Pure and Applied Chemistry (IUPAC), which is indicative of large pores. The adsorption continued to increase steadily during the medium-pressure (P/P_0 = 0.2-0.8) stage, revealing the wide size distribution (2-100 nm) of pores.[33] The inconsistent adsorption-desorption isotherm at P/P_0 = 0.3-1.0 was of H3 hysteresis loop, caused by capillary condensation of nitrogen in slit pores.[34] Although the particle size of the fly ash was less than 74 μm, the surface area and pore volume were lower (0.44 m^2 g^{-1} and 1.28 $10^{-3}cm^3$ g^{-1}, respectively) than that reported previously.[35] SEM images of the fly ash (Fig. S3) showed that the spherical morphology and the nonuniform particle size varied from 1 to 5 μm; nevertheless, pores were not obviously found except for the gap between particles.

Although the fly ash possessed only a small fraction (2.8 wt%) of CaO, the major content of SiO_2 and Al_2O_3 accounted for 78 wt% of the fly ash (Table S1), making it an abundant source of support materials for Ca-based sorbents. The mineral composition of the fly ash, especially the major content as expected based on the high T_T used for the sorbents,[36] was observed based on the XRD patterns (Fig. S4). The major crystalline materials were quartz (SiO_2, JCPDS 89-1961, 2θ = 20.83, 26.59 and 50.05° for the (1 0 0), (1 0 1) and (1 1 2) reflections, respectively) and mullite ($Al_{4.8}Si_{1.2}O_{9.6}$, JCPDS 79-1275, 2θ = 16.40, 26.17, 40.80° for the (1 1 0), (2 1 0) and (1 2 1) reflections, separately), along with a fraction of amorphous silica reflected by the broad diffraction peak at 2θ ≈ 22.46°.[37]

N_2 physisorption measurements revealed type II isotherms for both “CaO-2h” and “CaO-FA-2h” (Fig. S5 and S6), indicating the presence of micro- and mesopores. The BET surface area of the sorbents made from the calcium precursor of CaO was comparatively lower (1.33 and 1.29 m^2 g^{-1}, respectively, Table 1) than calcium D-gluconate (16.96 m^2 g^{-1}),[11] and showed a smaller total pore

volume (2.80 and 2.59 10^{-3}cm^3 g^{-1}, respectively). The H3 hysteresis loop was found only at P/P_0 = 0.4-1.0 for "CaO-2h", associated with the presence of slit pores.

The pore structure changed during the cyclic CO_2 capture according to the N_2 physisorption measurements for "CaO-2h" and "CaO-FA-2h" after the 4th and 29th cycle, separately (Fig. S5 and S6). Although the type of N_2 adsorption–desorption isotherm was not affected after cyclic CO_2 capture, both sorbents showed an extremely sharp increase in adsorption during the high-pressure stage (P/P_0 = 0.8-1.0) compared to the fresh sorbents, which was caused by intergranular gaps between the particles. The pore volume distributions of "CaO-2h" and "CaO-FA-2h" (Fig. 1) confirmed the pore structure changes, viz., the formation of numerous large pores (30-100 nm) after the 4th cycle. Thus, the total pore volume increased by 12.9-fold along with the average pore size for "CaO-FA-2h" after the 4th cycle (Table 1), which was possibly enlarged through the carbonation-calcination process.[14] "CaO-FA-2h" inevitably sintered in some degree under the severe calcination conditions, leading to a minor decrease in the BET surface area and the total pore volume after the 29th and 100th cycle. Similar structural changes were observed for "CaO-2h" during the first few cycles, however, the pore size further increased in subsequent cycles (the 29th and 100th cycle) due to the serious sintering without the stabilizer.[38]

Table 1 Summary of the structural parameters and the maximum sorption rates of the sorbents

Samples	Before cycle #	BET surface area (m^2 g^{-1})	Total pore volume (10^{-3} cm^3 g^{-1})	Average pore size (nm)	Max sorption rate dX dt^{-1} (10^{-3} s^{-1})	
					Carbonation	Calcination
CaO-2h	1st	1.33	2.80	7.57	2.29	-9.97
	5th [a]	4.98	44.17	26.16	4.23	-7.28
	30th	3.29	34.77	30.21	2.25	-3.74
	101th	1.26	19.26	52.21	1.93	-1.51
CaO-FA-2h	1st	1.29	2.59	7.68	1.89	-4.27
	5th	3.91	36.02	37.65	7.15	-4.95
	30th	3.69	30.02	24.86	3.84	-4.99
	101th	2.54	26.09	20.02	3.68	-4.83

[a] The sorbents before the 5th, 30th and 101th cycle were the same as those after the 4th , 29th and 100th cycle, separately.

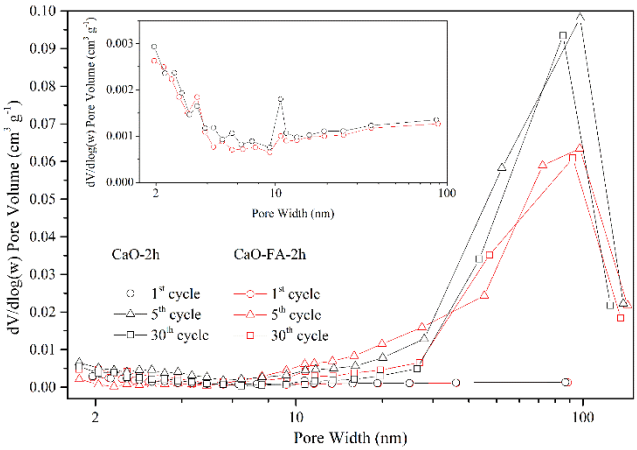

Fig. 1 Pore volume distributions of "CaO-2h" and "CaO-FA-2h" before the 1st, 5th, and 30th cycle, separately.

Fig. S7-(a) showed the particle (≈ 200 nm) morphology of "CaO-2h" with numerous pores on the surface, and the high-resolution TEM (HRTEM) image of "CaO-2h" (Fig. S7-(b)) showed the lattice image of CaO crystals. The TEM image of "CaO-FA-2h" showed comparatively larger particles (500-1000 nm) connected together, and the qualitative element mapping of Fig. 2-(b,c,d) further illustrated that the Ca element was uniformly distributed in the particles while the Si and Al elements were uniformly distributed only in the middle particle. Thus, we believe that the fly ash reacted with partial CaO and generated a new phase containing Ca, Si and Al, which was subsequently confirmed based on the XRD patterns. The new phase distributed uniformly and could effectively prevent the surrounded CaO particles, such as the particles on the two sides in Fig. 2-(a), from sintering together (Fig. 3-(f)).

Fig. 3 showed changes in the sorbent morphology during cyclic CO_2 capture. The SEM image of "CaO-2h" showed that nonuniform particles varied in size from 0.1-2 μm, which resulted in slit pores between the particles. The same particle morphology of CaO was also observed for "CaO-FA-2h" since it was synthesized through the physical dry-mixing of CaO and fly ash. However, some new angular crystal (insert of Fig. 3-(d)) was also found instead of the spherical particle of fly ash, which was indicative of the appearance of a new phase and verified by XRD patterns subsequently. Both "CaO-2h" and "CaO-FA-2h" were observed as larger particles (1-5 μm) with obvious surface cracks and more particle gaps (insert of Fig. 3-(b,e)) after the 4th cycle. Subsequently, the "CaO-2h" particles further enlarged up to 10-20 μm after the 29th cycle, leaving only a minor fraction of small particles adhered to the surface. However, the morphology of "CaO-FA-2h" was constant after the 29th cycle, indicating a slight sintering of CaO over the multiple carbonation-calcination.

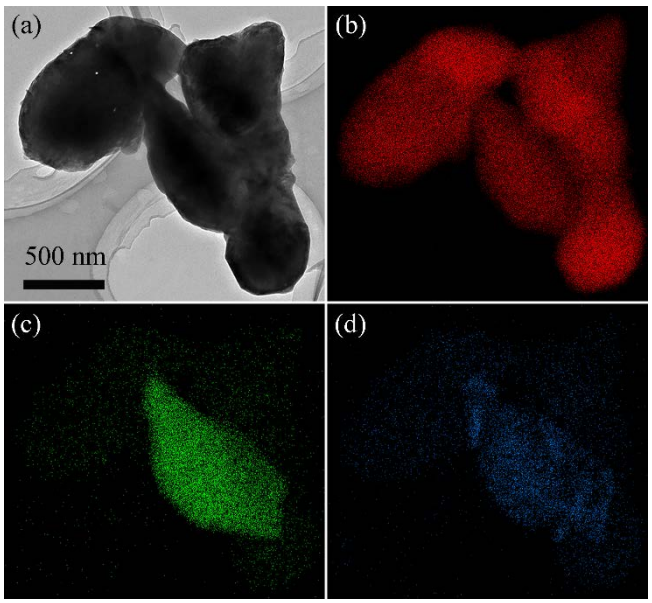

Fig. 2 (a) TEM images of "CaO-FA-2h"; Qualitative element mapping of (a) based on EELS analysis for (b) Ca, (c) Si, and (d) Al.

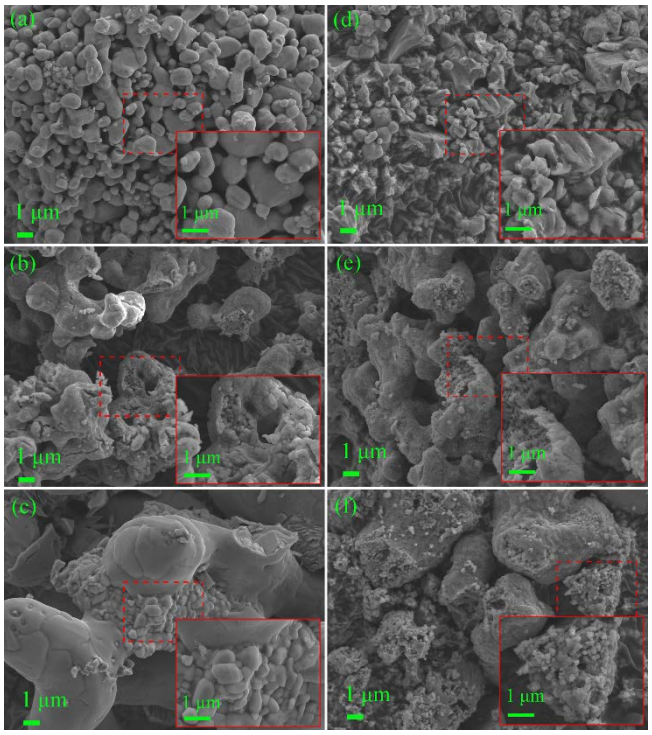

Fig. 3 SEM images of "CaO-2h" before the (a) 1st, (b) 5th and (c) 30th cycle; and "CaO-FA-2h" before the (d) 1st, (e) 5th and (f) 30th cycle. Magnification factor: ×5,000 for (a)-(f) and ×20,000 for the insertion of (a)-(f).

The XRD patterns of "CaO-2h" and "CaO-FA" exposed to various thermal treatment times (Fig. 4) showed primarily CaO crystals at 2θ = 32.20, 37.35 and 53.85°, which were assigned to (111), (200) and (220) reflections, respectively (JCPDS 37-1497). Normally, a fraction of CaO in the sorbents was air-slaked to $Ca(OH)_2$ crystal (JCPDS 01-1079, 2θ = 17.98, 34.06 and 47.05° for the (0 0 1), (1 0 1) and (1 0 2) reflections, separately) during the testing process. Not surprisingly,

"CaO-FA" without thermal treatment contained all crystalline phases of CaO and fly ash since "CaO-FA-0h" was physically mixed with CaO and fly ash.

However, the mineral composition of "CaO-FA" after thermal treatment (2, 6, and 12 h) changed, as expected based on the high calcination temperature of 950°C. The original crystalline phases of quartz and mullite were reduced or even disappeared, and a new crystalline phase, gehlenite ($Ca_2Al_2SiO_7$), was detected through the diffraction peaks at 2θ = 29.15, 31.43 and 52.12° for (2 0 1), (2 1 1) and (3 1 2) reflections, respectively (JCPDS 89-6887). Since there was little free corundum (Al_2O_3) in the fly ash and the presence of SiO_2 may also change the reaction mechanism, there were no relative reflections referring to Al_2O_3 or $Ca_{12}Al_{14}O_{33}$ (formed through reaction of CaO and Al_2O_3 at ~800°C).[27] Similar results have been reported by Cheng et al.,[39] in which the gehlenite phase formed at 850-1050°C from calcium-rich fly ash and showed better physical and mechanical properties at 900-950°C. Gehlenite generally exhibits good chemical durability as well as a high melting point of 1593°C (Table S2), which may be a good support to prevent sintering of Ca-based sorbent.

Although it was difficult to quantitatively analyze the CaO and $Ca_2Al_2SiO_7$ content due to the amorphous phase involved by fly ash, an obvious increase in the diffraction peaks referring to the $Ca_2Al_2SiO_7$ were observed as increasing the duration of thermal treatment. Besides, the phase change to form gehlenite continued throughout the cyclic carbonation-calcination process at 800-920°C, verified by the increase in the diffraction peaks for $Ca_2Al_2SiO_7$ (Fig. S9).

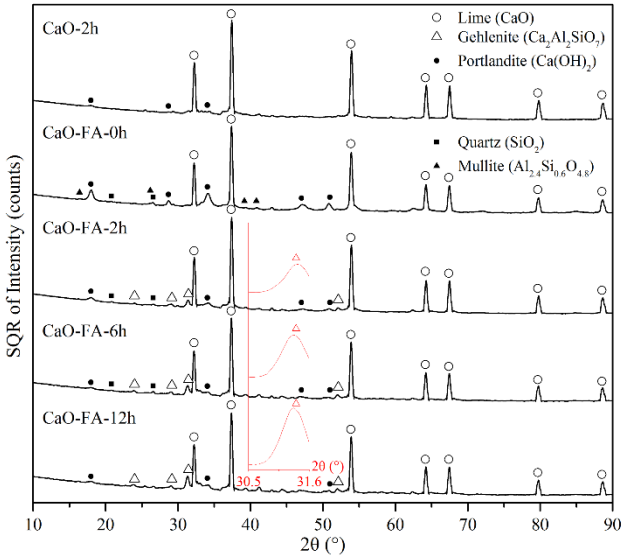

Fig. 4 XRD patterns of "CaO-2h", "CaO-FA-0h", "CaO-FA-2h", "CaO-FA-6h" and "CaO-FA-12h".

3.2 Cyclic CO_2 sorption

CO_2 uptake (X_N) was used to characterize the CO_2 capture capacity of CO_2 sorbents as a function of the number of carbonation−calcination cycles, N. Fig. 5-(a) plotted the CO_2 uptake in 30 cycles of the synthetic Ca-based sorbents (CaO-FA) and "CaO" after various thermal treatment times. "CaO-0h" possessed a high CO_2 uptake of 0.38 g(CO_2) g(sorbent)$^{-1}$ in the first cycle, which was in agreement with previous reports.[11] However, the CO_2 uptake decreased rapidly with cycle number to 0.14 and 0.076 g(CO_2) g(sorbent)$^{-1}$ after 10 and 30 cycles, respectively. Regarding synthetic sorbents, "CaO-FA-2h" possessed only a CO_2 uptake of 0.24 g(CO_2) g(sorbent)$^{-1}$ in the first cycle, significantly lower than that of "CaO-0h". Nevertheless, the CO_2 uptake interestingly increased to 0.28 g(CO_2) g(sorbent)$^{-1}$ after 5 cycles and processed a final CO_2 uptake of 0.21 g(CO_2) g(sorbent)$^{-1}$. Thus, the CO_2 capture capacity of "CaO-FA-2h" was markedly increased by 178% after 30 cycles than that of "CaO-0h", owing to the stabilizing effect of fly ash. Compared to the other Ca-based sorbents stabilized by solid-waste (Kaolin, Husk ash, and Cement) in Table 2, "CaO-FA" also resulted in a better cyclic stability considering the calcination condition and loss per cycle.

To clarify the effect mechanism of fly ash, "CaO-FA" with a preheating time of 0 to 12 h were tested by 30 cycles of carbonation-calcination. In the initial 10 cycles, the CO_2 uptake of "CaO-FA" decreased as the preheating time increased, which could be explained by two mechanisms. One was the chemical change of mineral compositions determined based on XRD patterns, in which more available CaO converted to the inert gehlenite as preheating time increased. The other was changes in the pore structure, including the particle growth and pore closure effects,[10] which could also explain the difference between "CaO-2h" and "CaO-0h". However, despite these large initial differences in CO_2 uptake, the behavior of "CaO-FA" (excluding "CaO-FA-0h") gradually converged after 30 cycles, because the sorbents did not maintain a memory of its previous calcinations and recarbonations, with regard to structural development and mineral composition.[40] For "CaO-FA-0h", the sintering of CaO and the formation of gehlenite occurred simultaneously; thus, part of the CaO sintered during the initial cycles without the isolation effect of gehlenite. Because the sintering of CaO was irreversible, the CO_2 uptake of "CaO-FA-0h" quickly decreased from 0.31 g(CO_2) g(sorbent)$^{-1}$ in the 5th cycle to 0.18 g(CO_2) g(sorbent)$^{-1}$ in the 30th cycle.

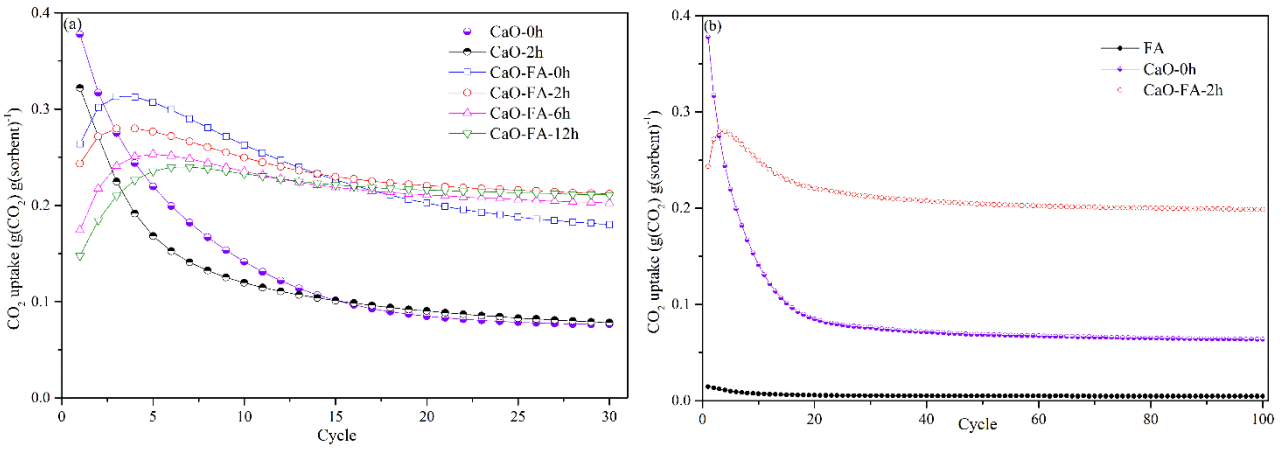

Fig. 5 (a) CO_2 uptake as a function of cycle for sorbents exposed to various thermal treatment times. (b) Extended CO_2 uptake of the selected sorbents: "FA", "CaO-0h" and "CaO-FA-2h". Conditions: Carbonation in 100 vol. % CO_2 at 800°C for 25 min and calcination in 100 vol. % CO_2 at 920°C for 5 min.

During the initial 5 cycles, the CO_2 uptake capacity of "CaO-FA" increased, indicating an effect of self-activation. To better characterize this phenomenon, the maximum rate of sorption ($dX\ dt^{-1}$, s^{-1}) was examined and summarized in Table 1. The carbonation reaction is usually comprised of two regimes: an initial fast carbonation stage controlled by surface reaction, associated with the filling of pore; and a subsequent significantly slower carbonation stage controlled by diffusion, in which a layer of $CaCO_3$ was deposited on the outer surface of the particles.[41] Fig. 6, which showed the CO_2 uptake and reaction temperature as a function of time, demonstrated clearly that the CO_2 uptake of the sorbents occurred mostly in the fast carbonation stage, except for the first cycle.

In the first cycle, CO_2 uptake in the sorbents did not occur in distinct fast and slow stages, as is usually observed,[27] but rather occurred gradually over the entire 25-min period. This phenomenon could be attributed to the small pore size and limited pore volumes which restricted the diffusion process, but it would become easier as the pore size would be enlarged by the supports during the initial cycles (Fig. 1). Thus, the maximum rate of carbonation for "CaO-FA-2h" increased significantly from 1.89 s^{-1} in the 1st cycle to 7.15 s^{-1} in the 5th cycle due to structural changes and the formation of cracks and pores (Fig. 3-(d)), which are convenient for fast carbonation.[42] Subsequently, the maximum rate of carbonation decreased to 3.84 s^{-1} along with the CO_2 uptake in the 30th cycle due to (i) slight sintering leading to the decrease of pore volume (Table 1) and (ii) continuous formation of gehlenite (Fig. S9), which is inert with regard to CO_2 capture. The maximum calcination rate for "CaO-FA-2h" was similar, indicating that the fundamental mesopore structure was well-maintained during the cyclic CO_2 uptake.

Since the transition from the fast to slow carbonation stage occurred once the $CaCO_3$ product

layer exceeded a thickness of ~50 nm,[43] maintaining the nanostructure of the sorbents could minimize the extent of the slow, diffusion limited reaction regime of the carbonation. Therefore, the uniformly dispersed support (gehlenite) with high melting point, which ensured stability of the nanostructured morphology, played a crucial role in stable CO_2 capture capacity of the synthetic sorbents over multiple reaction cycles. On the other hand, "CaO-2h" rapidly lost its nanostructured morphology due to the severe sintering, resulting in the formation of large particles and voids (Fig. 3-(b, c)) during the initial cycles. Because the small pores in the fresh sorbent was not enlarged but disappeared without supports, the CO_2 uptake and maximum calcination rate decreased as the cycle increased, although the same variation trend of the maximum carbonation rate was observed.

Table 2 Synthetic Ca-based sorbents: Effectiveness and stability over cycles of carbonation and calcination

Support	CaO content (wt%)	Carbonation			Calcination			N, Cycles	$X_{residue}$ [b] ($g(CO_2)$ $g(sorbent)^{-1}$)	Loss [c] (%)
		T (ºC)	t (min)	CO_2 [a] (%)	T (ºC)	t (min)	CO_2 [a] (%)			
FA	**90**	**800**	**25**	**100**	**920**	**5**	**100** [k]	**100**	**0.20**	**0.18**
Kaolin [d, 29]	90	650	20	15	920	10	100 [k]	30	0.13	1.47
Husk ash [e, 30]	84	700	15	15	850	20	0	50	0.27	0.78
Cement [e, 31]	75	650	30	15	900	10	0	18	0.23	1.89
Al_2O_3 [f, 14]	91	750	20	100	750	20	0	30	0.56	-0.12 [j]
Al_2O_3 [26]	91	750	20	100	750	20	0	30	0.51 [g]	0.29
		750	20	100	750	20	0	30	0.31 [d]	1.67
Al_2O_3 [e, 27]	91	750	20	20	750	20	0	10	0.49	-0.89 [j]
		650	20	20	900	10	100 [k]	10	0.28	2.82
MgO [f, 17]	71	750	20	50	750	20	0	15	0.51	0.60
MgO [h, 18]	75	650	30	15	900	10	0	24	0.56	0.21
Nano-SiO_2 [e, 19]	85	650	5	15	850	5	0	100	0.18	0.65
Ca_2SiO_4 [d, 20]	89	650	30	15	850	10	0	15	0.52	0.10
ZrO_2 [i, 21]	84	675	20	100	850	10	0	20	0.32	1.54
TiO_2 [i, 23]	41	650	120	66	850	60	0	28	0.15	1.93
Y_2O_3 [f, 25]	14.3	740	10	50	740	10	0	100	0.08	0.02

[a] The content of CO_2 in the atmosphere was adjusted by N_2. [b] X_1 and $X_{residue}$ refer to the CO_2 uptake in the first and last cycle, separately. [c] The average change in CO_2 uptake capacity per cycle: $(1-X_{residue}/X_1)/N*100\%$. [d] The calcium precursor was $Ca(Ac)_2$. [e] The calcium precursor was $Ca(OH)_2$. [f] The calcium precursor was $Ca(NO_3)_2$. [g] The calcium precursor was $Ca(C_5H_7O_2)_2$. [h] The CaO precursor was calcium D-gluconate monohydrate. [i] The CaO precursor was $CaCO_3$. [j] The CO_2 uptake capacity increased initially. [k] When the calcination atmosphere was pure CO_2, there was a slight increase in CO_2 uptake during the switch from carbonation to calcination, which was called "recarbonation".

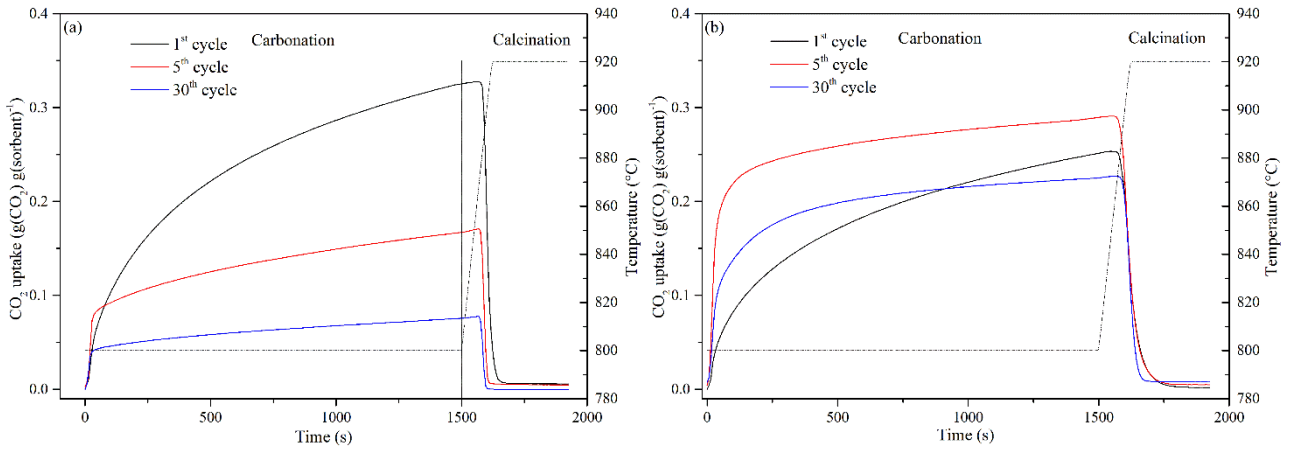

Fig. 6 CO_2 uptake and reaction temperature as a function of reaction time for (a) "CaO-2h" and (b) "CaO-FA-2h" during the 1st, 5th, and 30th cycle, separately.

To investigate the effect of fly ash on the long-term stability of the Ca-based sorbents, extended carbonation-calcination cycles (100 cycles) were performed for "FA", "CaO-0h" and "CaO-FA-2h" (Fig. 5-(b)). Not surprisingly, CO_2 capture capacity of "FA" was negligible (less than 0.01 g(CO_2) g(sorbent)$^{-1}$), as the alkali earth metal oxide content of fly ash was 7.6%. Similarly to the 30-cycles runs (Fig. 5-(a)), "CaO-FA-2h" showed the highest stability at the 100th cycle, 0.20 g(CO_2) g(sorbent)$^{-1}$, with a slight drop compared to the 30th cycle, 0.21 g(CO_2) g(sorbent)$^{-1}$. The average deactivation rate of "CaO-FA-2h" over the 100 cycles was merely 0.18% per cycle and even lowered to 0.086% per cycle for the last 70 cycles. This is much better performance than that of "CaO-0h", 0.83% per cycle. In terms of the net capture capacity upon the 100th cycle, "CaO-FA-2h" performed 211% better than "CaO-0h" (0.064 g(CO_2) g(sorbent)$^{-1}$).

CO_2 uptake of Ca-based sorbents is generally influenced by the calcium precursor, the carbonation temperature and the calcination conditions. CaO derived from calcium organic acid usually had a higher surface area and pore volume, and thus a higher CO_2 uptake.[11] A major difference of calcium precursor for CO_2 uptake was observed by Broda et al. (Table 2),[26] in which the CO_2 uptakes were 0.31 and 0.51 g(CO_2) g(sorbent)$^{-1}$ for the Al_2O_3-stabilized sorbents using $Ca(Ac)_2$ and $Ca(C_5H_7O_2)_2$, respectively. Since a temperature > 900ºC is required for calcination under pure CO_2 atmosphere, the higher carbonation temperature is desirable to minimize the temperature change over the cycle. Although, the lower temperature and lower CO_2 partial pressure plays a crucial role in slowing the sintering of sorbents.[44] Broda et al.[27] reported a stable Al_2O_3-stabilized sorbent (Table 2) with a CO_2 uptake of 0.49 g(CO_2) g(sorbent)$^{-1}$ after 10 cycles, which was quite a pleased result. However, it sharply decreased to 0.28 g(CO_2) g(sorbent)$^{-1}$ when

the calcination condition changed to 900ºC under a pure CO_2 atmosphere. When the calcination atmosphere was pure CO_2, there was a sl ight increase in CO_2 uptake during the switch from carbonation to calcination (see Fig. 6), since the conversion of CaO increases with the increasing of temperature.[45] This process, so-called "recarbonation", will increase cyclic capacity as is reported by Valverde et al.,[46] however, the positive effect of recarbonation is far from offsetting the rapid decay of CO_2 uptake under the severe calcination conditions. Regarding "CaO-FA-2h", the high-temperature stability (loss rate of 0.18% per cycle) under the severe calcination condition was extremely encouraging, despite the comparatively low CO_2 uptake in the 1st cycle. We can change the calcium precursor and carbonation temperature to enhance the initial CO_2 uptake; however, the total cost for per ton CO_2 avoided should be calculated and compared. Since the Ca-based sorbents would be calcined in an atmosphere of around 100% CO_2 in real cyclic carbonation-calcination systems,[47] the as-synthesized fly-ash-stabilized CaO sorbents are more promising for scaled up applications.

4. Conclusion

An economical and environment-friendly strategy was developed to reduce sintering of CaO by recycling solid waste (fly ash) as a stabilization additive to Ca-based sorbents. The effect of fly ash on the multi-cycle stability of Ca-based sorbents at high temperatures was firstly reported on basis of several analytical techniques. It was found that a new phase (gehlenite) with high melting point formed during calcination at 950ºC and mitigated CaO crystal grains from sintering. Despite the relatively low initial CO_2 uptake (0.24 g(CO_2) g(sorbent)$^{-1}$) owing to the cheap calcium precursor, the as-synthesized sorbent, "CaO-FA-2h", possessed a CO_2 uptake of 0.20 g(CO_2) g(sorbent)$^{-1}$ after 100 cycles and a particularly low average deactivation rate of 0.18% per cycle. Considering the extremely severe calcination (920ºC in pure CO_2 atmosphere), which is compatible with the real cyclic carbonation-calcinations system, we conclude that this easily approachable new sorbent material is promising for scaled-up CO_2 capture from both economic and environmental points of view.

Electronic supplementary information (ESI)

Table S1-S2 and Fig. S1–S9 are included in the ESI.

Acknowledgements

The authors gratefully acknowledge the Hi-Tech Research and Development Program (863) of China for financial

support (grant no. 2012AA06A116).

Reference

1 IPCC, 2013: Climate change 2013: The physical science basis. Contribution of working group I to the fifth assessment report of the intergovernmental panel on climate chang. Cambridge university press, cambridge, United Kingdom and New York, NY, USA, 1535 pp.

http://www.climatechange2013.org/images/report/WG1AR5_ALL_FINAL.pdf

2 S. Pacala and R. Socolow, *Science*, 2004, **305**, 968-972.

3 P. H. Stauffer, G. N. Keating, R. S. Middleton, H. S. Viswanathan, K. A. Berchtold, R. P. Singh, R. J. Pawar and Anthony Mancino, *Environ. Sci. Technol.*, 2011, **45**, 8597-8604.

4 T. Shimizu, T. Hirama, H. Hosoda, K. Kitano, M. Inagaki and K. Tejima, *Chem.Eng. Res. Des.*, 1999, **77**, 62-68.

5 M. Zhao, A. I. Minett and A. T. Harris, *Energy Environ. Sci.*, 2013, **6**, 25-40.

6 M. E. Boot-Handford, J. C. Abanades, E. J. Anthony, M. J. Blunt, S. Brandani, N. Mac Dowell, J. R. Fernandez, M.-C. Ferrari, R. Gross, J. P. Hallett, R. S. Haszeldine, P. Heptonstall, A. Lyngfelt, Z. Makuch, E. Mangano, R. T. J. Porter, M. Pourkashanian, G. T. Rochelle, N. Shah, J. G. Yao and P. S. Fennell, *Energy Environ. Sci.*, 2014, **7**, 130-189.

7 Q. Wang, J. Z. Luo, Z. Y. Zhong and A. Borgna, *Energy Environ. Sci.*, 2011, **4**, 42-55.

8 N. MacDowell, N. Florin, A. Buchard, J. Hallett, A. Galindo, G. Jackson, C. S. Adjiman, C. K. Williams, N. Shah and P. Fennell, *Energy Environ. Sci.*, 2010, **3**, 1645-1669.

9 V. Manovic and E. J. Anthony, *Environ. Sci. Technol.*, 2007, **41**, 1420-1425.

10 V. Manovic and E. J. Anthony, *Environ. Sci. Technol.*, 2008, **42**, 4170-4174.

11 W. Liu, N. W. Low, B. Feng, G. Wang and J. C. Diniz da Costa, *Environ. Sci. Technol.*, 2010, **44**, 841-847.

12 E. T. Santos, C. Alfonsfn, A. J. S. Chambel, A. Fernandes, A. P. Soares Dias, C. I. C. Pinheiro and M. F. Ribeiro, *Fuel*, 2012, **94**, 624-628.

13 G. Grasa, B. Gonzlez, M. Alonso and J. C. Abanades, *Energy Fuels*, 2007, **21**, 3560-3562.

14 M. Broda and C. R. Müller, *Advanced Materials*, 2012, **24**, 3059-3064.

15 P. H. Chang, Y. P. Chang, S. Y. Chen, C. T. Yu and Y. P. Chyou, *ChemSusChem*, 2011, **4**, 1844-1851.

16 Y. P. Chang, Y.C. Chen, P.H. Chang and S. Y. Chen, *ChemSusChem*, 2012, **5**, 1249-1257.

17 R. Filitz, A. M. Kierzkowska, M. Broda and C. R. Müller, *Environ. Sci. Technol.*, 2012, **46**, 559-565.

18 W. Q. Liu, B. Feng, Y. Q. Wu, G.X. Wang, J. Barry and J. C. Diniz Da Costa, *Environ. Sci. Technol.*, 2010, **44**, 3093-3097.

19 J. M. Valverde, A. Perejon and L. A. Perez-Maqueda, *Environ. Sci. Technol.*, 2012, **46**, 6401-6408.

20 M. Zhao, J. Shi, X. Zhong, S. C. Tian, J. Blamey, J. G. Jiang and P. S. Fennell, *Energy Environ. Sci.*, 2014, **7**, 3291-3295.

21 Z. K. Sun, M. H. Sedghkerdar, J. Saayman, N. Mahinpey, N.K. Ellis, D. Y. Zhaod and S. Kaliaguine, *J. Mater. Chem. A*, 2014, **2**, 16577-16588.

22 M. Zhao, M. Bilton, A. P. Brown, A. M. Cunliffe, E. Dvininov, V. Dupont, T. P. Comyn and S. J. Milne, *Energy Fuels*, 2014, **28**, 1275-1283.

23 L. Vieille, A. Govin and P. Grosseau, *Powder Technol.*, 2012, **228**, 319-323.

24 S. F. Wu and Y. Q. Zhu, *Ind. Eng. Chem. Res.*, 2010, **49**, 2701-2706.

25 V. S. Derevschikov, A. I. Lysikov and A. G. Okunev, *Ind. Eng. Chem. Res.*, 2011, **50**, 12741-12749.

26 M. Broda, A. M. Kierzkowska and C. R. Müller, *ChemSusChem*, 2012, **5**, 411-418.

27 M. Broda, A. M. Kierzkowska and C. R. Müller, *Environ. Sci. Technol.*, 2012, **46**, 10849-10856.

28 Z. S. Li, N. S. Cai, Y. Y. Huang and H. J. Han, *Energy Fuels*, 2005, **19**, 1447-1452.

29 F. N. Ridha, V. Manovic, A. Macchi and E. J. Anthony, *Int. J. Greenhouse Gas Control*, 2012, **6**, 164-170.

30 Y. Li, C. Zhao, Q. Ren, L. Duan, H. Chen and X. Chen, *Fuel Process. Technol.*, 2009, **90**, 825-834.

31 C. Qin, J. J. Yin, H. An, W. Q. Liu and B. Feng, *Energy Fuels*, 2012, **26**, 154-161.

32 Y. Z. Chen, N. Shah, F. E. Huggins and G. P. Huffma, *Environ. Sci. Technol.*, 2005, **39**, 1144-1151.

33 J. X. Jiang, J. H. Yu and A. Corma, *Angew. Chem. Int. Ed.*, 2010, **49**, 3120-3145.

34 Q. Yue, M. H. Wang, J. Wei, Y. H. Deng, T.Y. Liu, R. Che, B. Tu and D. Y. Zhao, Angew. *Chem. Int. Ed.*, 2012, **51**, 10368-10372.

35 H. H. Chen, A. Laskin, J. Baltrusaitis, C. A. Gorski, M. M. Scherer and V. H. Grassian, *Environ. Sci. Technol.*, 2012, **46**, 2112-2120.

36 S. B. Wang, *Environ. Sci. Technol.*, 2008, **42**, 7055-7063.

37 F. Hoffmann, M. Cornelius, J. Morell and M. Fröba, *Angew. Chem. Int. Ed.*, 2006, **45**, 3216-3251.

38 V. Manovic and E. J. Anthony, *Environ. Sci. Technol.*, 2009, **43**, 7117-7122.

39 T. W. Cheng and Y. S. Chen, *Chemosphere*, 2003, **51**, 817-824.

40 V. Manovic, E. J. Anthony, G. Grasa and J. C. Abanades, *Energy Fuels*, 2008**, 22**, 3258-3264

41 J. Blamey, E. J. Anthony, J. Wang and P. S. Fennell, *Prog. Energy Combust. Sci.*, 2010, **36**, 260-279.

42 N. J. Amos, M. Widyawati, S. Kureti, D. Trimis, A. I. Minett, A. T. Harris and T. L. Church, *J. Mater. Chem. A*, 2014, **2**, 4332-4339.

43 D. Alvarez and J. C. Abanades, *Ind. Eng. Chem. Res.*, 2005, **44**, 5608-5615.

44 A. M. Kierzkowska, R. Pacciani and C. R. Müller, *ChemSusChem*, 2013, **6**, 1130-1148.

45 Z. S. Li, F. Fang, X. Y. Tang and N. S. Cai, *Energy Fuels*, 2012, **26**, 2473-2482.

46 J. M. Valverde, P. E. Sanchez-Jimenez, L. A. Perez-Maqueda M. A. S. Quintanilla, J. Perez-Vaquero, *Applied Energy*, 2014, **125**, 264-275.

47 C. Qin, W. Q. Liu, H. An, J. J. Yin and B. Feng, *Environ. Sci. Technol.*, 2012, **46**, 1932-1939.